# "Z" and "qZ" Source Inverters as Electronic Ballast

Nimrod Vázquez, *Senior Member, IEEE*, Edgar Baeza, Alejandro Perea, Claudia Hernández, *Member, IEEE*, Eslí Vázquez, and Héctor López

***Abstract*—Electronic ballasts are implemented for obtaining a high power factor and a good operation of the lamp; these goals are reached traditionally by implementing multiple stages. On the first stage, a unity power factor is obtained and the second stage is designed in order to feed properly the lamp. Different topologies have been studied not only for decreasing the number of employed controllers and stages, but also reducing the number of components and active switches. Electronic ballasts, which are based on the "Z" and "qZ" source inverters, are considered in this paper, where the proposed systems have a single stage. Two topologies are illustrated: the first one for the fluorescent lamps and the second one for the high intensity discharge lamps, where electronic ballasts with a high power factor are obtained. The operation, analysis, and experimental results are shown.**

***Index Terms*—Electronic ballast, impedance inverter, power factor correction.**

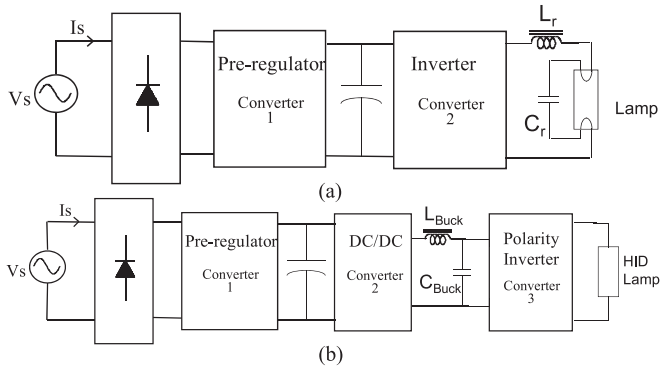


Fig. 1. Electronic ballast. (a) Two-stage approach for fluorescent lamp. (b) Three-stage approach for HID lamp.

## I. Introduction

ELECTRONIC ballasts are widely used by the fluorescent and high intensity discharge (HID) lamps due to its good performance such as high efficiency, high power factor (PF), and light weight. Different topologies are found published in the literature [1]–[21] for each type of lamp, traditionally a two stage topology applies for the fluorescent lamps, as shown in Fig. 1(a), while a three-stage topology is found implemented for the HID lamps, as illustrated in Fig. 1(b).

Both the power quality and the proper lamp operation have become the requirements to be fulfilled by the electronic ballast. Particularly in a two-stage approach, each requirement is separately fulfilled in every stage. However, this scheme requires a considerable amount of semiconductors, which diminish the efficiency. Different choices have been proposed in order to reduce the drawbacks for the two-stage approach in each type of the lamp.

Manuscript received September 27, 2015; revised December 11, 2015; accepted January 09, 2016. Date of publication January 19, 2016; date of current version June 24, 2016. This work was supported by Dirección General de Educación Superior Tecnológica. Recommended for publication by Associate Editor H. Cha.

N. Vázquez, C. Hernández, and H. López are with the Department of Electronics Engineering, Instituto Tecnológico de Celaya, Celaya 38010, México (e-mail: n.vazquez@ieee.org; claudia.hernandez@itcelaya.edu.mx; hector.lopez@itcelaya.edu.mx).

E. Baeza was with the Instituto Tecnológico de Celaya, Celaya 38010, México. He is now with the Department of Engineering, Universidad Tecnológica del Norte de Guanajuato, Dolores Hidalgo 37800, México (e-mail: ebaezatrejo@gmail.com).

A. Perea was with the Instituto Tecnológico de Celaya, Celaya 38010, México. He is now with the Company Mariscala P&G and Nestlé-Purina, León 37290, México (e-mail: pereagol@yahoo.com.mx).

E. Vázquez is with the Engineering Faculty, Universidad de Veracruz, Boca del Rio 94294, México (e-mail: evazquezn@gmail.com).

Color versions of one or more of the figures in this paper are available online at http://ieeexplore.ieee.org.

Digital Object Identifier 10.1109/TPEL.2016.2519393

There exist a variety on the proposed topologies for the fluorescent lamps; there are integrated topologies [1]–[7], some are based on the charge pump technique [8]–[10], some others are made magnetically [11]–[13], and also some other proposals [14], [15] suggest a self-oscillating converter.

It is also normally found in the literature [16]–[21] three-stage ballast circuit for HID lamps. It consists of a boost converter for PFC, a buck converter for regulating lamp power, and a full-bridge inverter. There also exists a two-stage low-frequency square-wave-driven ballast circuit [16], [17].

Electronic ballasts based on "Z" and "qZ" source inverters, for a fluorescent lamp and an HID lamp, respectively, are proposed in this paper. The described systems in this paper offer a good PF and a proper lamp operation.

Both "Z" and "qZ" source inverters have a higher amount of switching states than conventional inverters; this extra configuration is called shoot-through state. Thus, it is used in this paper not only to boost the input voltage as traditionally is employed [22]–[26], but also to correct the PF. Neither more stages nor the converter integration is required in order to achieve both functions: the high PF correction and proper lamp operation.

On one side, it is proposed to operate the inductor for the "Z" source inverter in a similar way to discontinuous conduction mode (DCM), so that, a high PF is obtained in natural form. On the other side, it is proposed to operate the inductor for the "qZ" topology in a continuous conduction mode (CCM), as consequence a resistance emulator controller is required, therefore, both lower current stress and the output power may be increased.

The conduction mode selected for each topology is due to the natural operating mode, this means that, the first topology demands a discontinuous current and the second one a continuous current, so that, this was considered for selecting the conduction mode for both the converters, and the shoot-through state is not only employed just for the purpose of boosting.

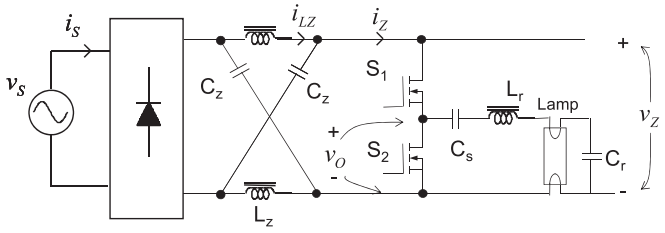


Fig. 2. Electronic ballast based on "Z" source inverter.

This paper is organized as follows: proposed converters are addressed in Section II, where, it is described not only operation and waveforms but also analysis about the proposals is included. Experimental results are discussed in Section III, and the final conclusion is given.

## II. "Z" and "qZ" Electronic Ballast

Voltage and current source inverters (VSI and CSI, respectively,) are the inverters normally found in the literature [1]–[21], which are employed in the electronic ballast. The "Z" source inverter (ZSI) found is also considered in the literature [22].

ZSI, in comparison with both the CSI and VSI, allows blanking time and overlapping time in one inverter leg; particularly, this feature allows us to operate this inverter with more switching states, therefore, the possibilities in its functionality are better.

This advantage has been applied in this paper in order to satisfy the two requirements (power quality standard and current crest factor) by the electronic ballast with a single stage. While some switching states are used in order to control the lamp output voltage, some other states are used for satisfying specifications for the input current; all of these together make the lamp operate properly.

Although, the "Z" source topology is used for a fluorescent lamp, and the "qZ" source converter for an HID lamp, they may be used indistinctly, with their own respective considerations.

### A. Electronic Ballast Based on ZSI

The converter consists of two active semiconductors, the passive elements, and the full-bridge rectifier, as shown in Fig. 2. It is easily seen that just one leg is considered of an inverter. The output voltage is a square waveform, which is filtered by a series–parallel resonant tank and applied to the fluorescent lamp.

The converter may also be seen as a combination of a half-bridge resonant inverter and the Z-source; this allows us to have more switching states, so that, it gives more possibilities in the inverter functionality, as for example, the PF correction without the integration of other converter or stages.

According to Fig. 3, the converter operates as follows:

1) *During* $t_0$–$t_1$. $S_1$ and $S_2$ are turned ON, the equivalent subcircuit is shown in Fig. 4(a), and then a zero voltage is applied to the resonant tank; it should be noticed that the full bridge diode is not conducting, and then the current of the ac mains is zero.
2) *During* $t_1$–$t_2$. $S_1$ is maintained ON, $S_2$ is turned OFF, the equivalent subcircuit is shown in Fig. 4(b), and then a positive output voltage is delivered to the resonant tank; the full-bridge diode is conducting until the input current reaches the zero current and then the full bridge diode is open; after that finishes this stage.
3) *During* $t_2$–$t_3$. $S_1$ is still ON, but also $S_2$ is OFF, the equivalent subcircuit is shown in Fig. 4(c), a positive output voltage is still delivered to the resonant tank; the current of the "Z" inductor is the half of the resonant tank inductor current.
4) *During* $t_3$–$t_4$. $S_1$ is turned ON and $S_2$ is turned OFF, the equivalent subcircuit is shown in Fig. 4(d), and then a zero voltage is applied to the resonant tank. The current of the "Z" inductor is discharged to the capacitor through the full-bridge diodes, and then a current appears at the ac mains. This stage finishes until this current reach the zero value.
5) *During* $t_4$–$t_5$. $S_1$ is maintained ON and also $S_2$ is maintained OFF, the equivalent subcircuit is shown in Fig. 4(e), and then a zero voltage is applied to the resonant tank. No current at "Z" inductor and ac mains.
6) *After* $t_5$. The switching sequences are being repeated since this time.

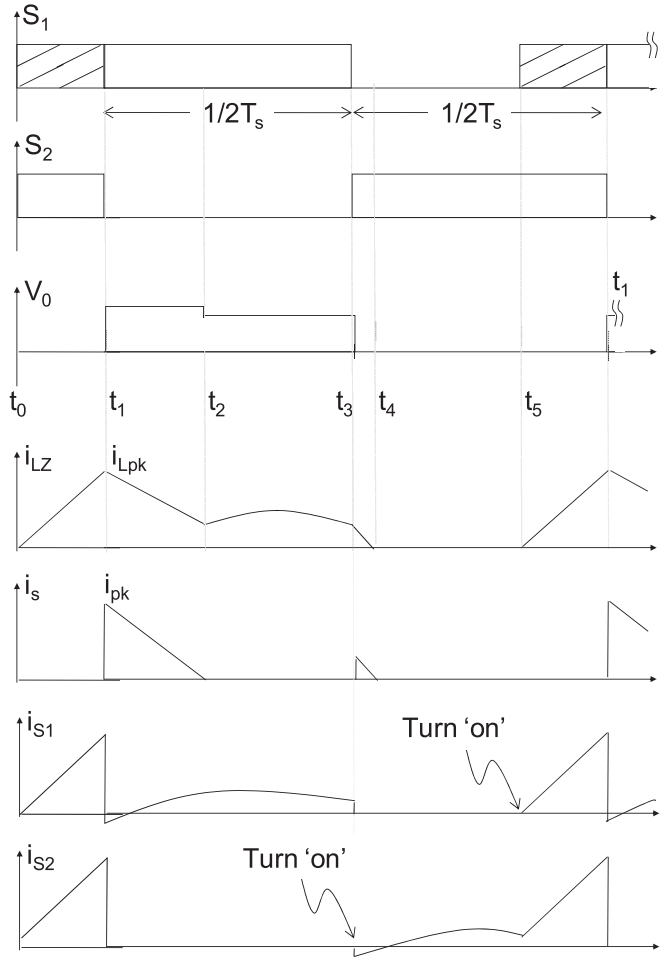


Fig. 3. Output waveform of the ZSI at one switching period.

It should be noticed that the waveforms illustrated in Fig. 3 are at high frequency and does not include the electromagnetic

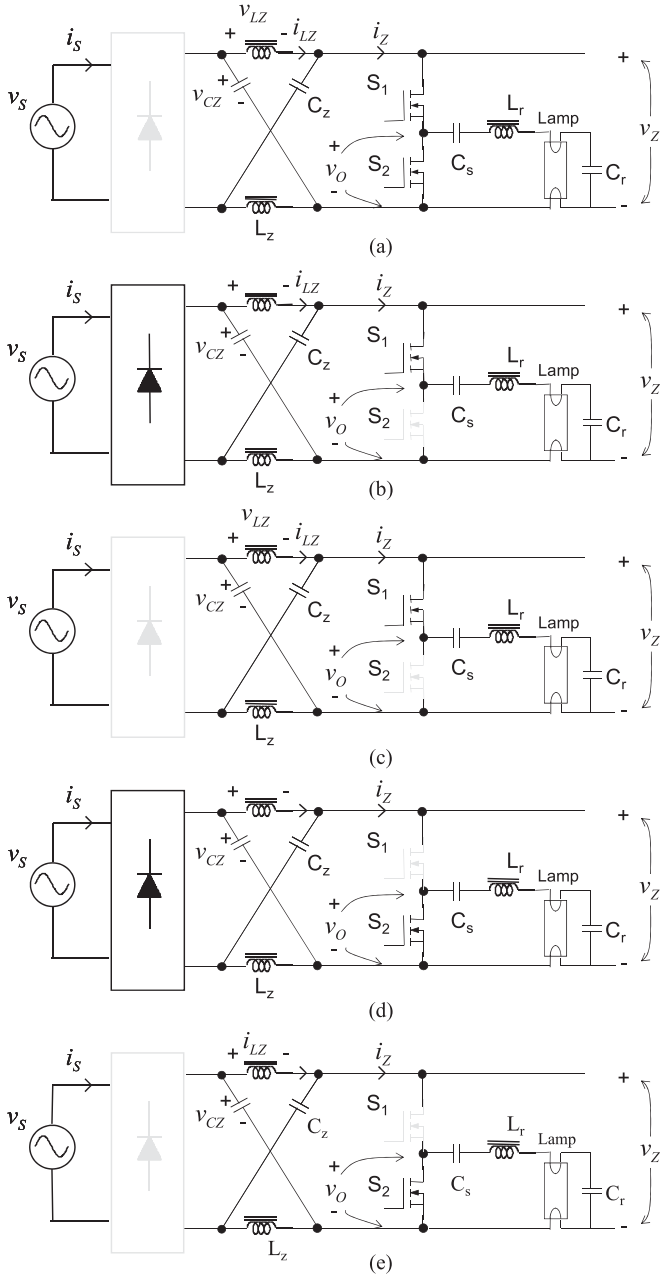


Fig. 4. Subcircuits of the first proposed converter.

interference filter at the ac mains, which it is required for this type of operation. This is explained because the converter is operated in a DCM.

Different switching states for producing the required output voltage are summarized in Table I. The reader should be aware that there exist more switching states than those for the traditional inverter in order to generate zero output voltage; this redundancy is used to correct the PF.

The current for the two switches is shown at the bottom of Fig. 3, it should be noticed that when they are turned "ON," the current starts from zero or from a negative value, so that, a soft switching is performed in both switches; however, it does not occur when they are turned "OFF."

TABLE I
SWITCHING STATES OF THE Z CONVERTER

| Output voltage | Switches | | |
|---|---|---|---|
| | $S_1$ | $S_2$ | "1" means "ON" |
| Zero | 1 | 1 | "0" means "OFF" |
| | 0 | 1 | |
| Positive | 1 | 0 | |

*1) Output Characteristics:* The output for this proposed inverter stage is a square output voltage, so that, in order to obtain an ac output voltage, a series–parallel resonant tank is considered.

The resonant tank is made with $C_s, L_r$, and $C_r$. Since the resonance, between $L_r$ and $C_r$, does not change, $C_s$ is selected typically ten times higher than $C_p$ [18], as a result $C_s$ is used only to suppress the CD component. Therefore, the following equation may be used for the design:

$$\omega_d = \frac{1.1}{\sqrt{L_r C_r}} \tag{1}$$

$$P_{OL} = \frac{\left(\frac{R}{\omega_d L_r}\frac{4V_{\mathrm{dc}}}{\pi}\right)^2}{2R} \tag{2}$$

where $L_r$ and $C_r$ are the inductance and capacitance of the resonant tank, *R* is the lamp resistance in steady state, and $\omega_d$ is the desired output voltage frequency.

*2) Input Characteristics:* The inverter input is the "Z" array and also the full-bridge rectifier. A high PF is obtained due to inductors $L_Z$, which are operated as in a DCM.

According to the input current waveform, this converter operates very similar as it is done by a parallel active input current shaper found in the literature [27]; however, its topology is completely different.

Related equations to the input are obtained during $t_1$–$t_2$. Particularly, for the analysis, it is considered that the capacitor voltages and the ac mains are almost constant in a switching period.

The voltage applied to the $L_Z$ inductor [see Fig. 4(b)] is determined by

$$v_{LZ} = |v_S| - v_{CZ} \tag{3}$$

where: $v_{CZ}$ is the capacitor voltage of $C_Z$;
$|v_S|$ is the rectified ac mains.

Also from the same figure the input current is

$$|i_S| = 2i_{LZ} - i_Z \tag{4}$$

where: $i_{LZ}$ is the inductor current of $L_Z$;
$i_Z$ is the current demanded by the inverter.

By considering expression (4), then for the instant $t_1$, the input current may be approximated to

$$i_{pk} = 2i_{Lpk} - i_{Zt1} \tag{5}$$

where $i_{Lpk}$ is the inductor current of $L_Z$ at the time $t_1$, $i_{pk}$ is the current demanded by rectified ac mains at the time $t_1$, and $i_{Zt1}$ is the current demanded by the inverter at the time $t_1$.

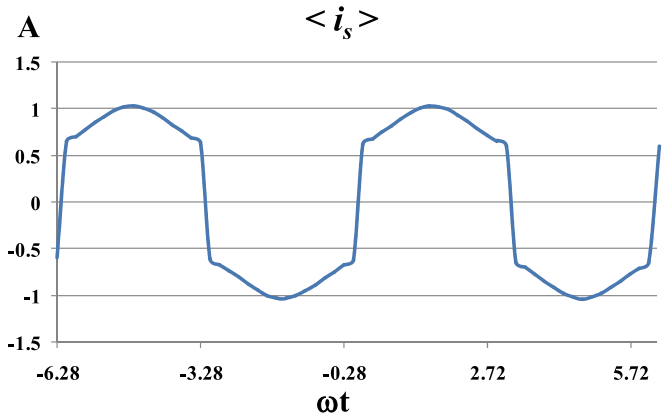


Fig. 5. Theoretical waveform of the input current.

From the Fig. 4(b), the basic equation for the inductor may be obtained as

$$\frac{i_{Zt2} - i_{Lpk}}{t_2 - t_1} = -\frac{v_{LZ}}{L_Z} \tag{6}$$

where $i_{Zt2}$ is the current demanded by the inverter at the time $t_2$.

The following equations may be deduced by assuming that the current demanded by the inverter is smaller in comparison to the peak of the input or inductor currents:

$$i_{pk} = 2i_{Lpk} \tag{7}$$

$$\frac{-i_{Lpk}}{t_2 - t_1} = -\frac{v_{LZ}}{L_Z}. \tag{8}$$

Then, by using (3), (7), and (8):

$$t_2 - t_1 = \frac{i_{pk} L_Z}{2\left(|v_S| - v_{CZ}\right)}. \tag{9}$$

The average current at the high frequency is obtained as

$$\langle i_S \rangle = \frac{1}{T_s} \int_{-(t_2 - t_1)}^{0} -\frac{i_{pk}}{t_2 - t_1} t \, dt. \tag{10}$$

Substituting (9) in (10) and solving, we obtain

$$\langle i_S \rangle = \frac{1}{T_s} \int_{-(t_2 - t_1)}^{0} -\frac{2\left(|v_S| - v_{CZ}\right)}{L_Z} t \, dt$$

$$\langle i_S \rangle = \frac{1}{T_s} \frac{2\left(v_{CZ} - |v_S|\right)}{L_Z} \left(t_2 - t_1\right)^2. \tag{11}$$

Substituting (9) in (11) we obtain

$$\langle i_S \rangle = \frac{1}{T_s} \frac{i_{pk}^2 L_Z}{2\left(v_{CZ} - |v_S|\right)}. \tag{12}$$

If the time $t_1$–$t_0$ is maintained constant, then $i_{pk}$ is constant, so that, the evolution of the average current $\langle i_S \rangle$ depends on the variations of the ac mains. The waveform shown in Fig. 5 is obtained by graphing expression (12), the result is similar to this obtained by the parallel active input current shaper [27], which offers a good PF, however, not equal to the unity.

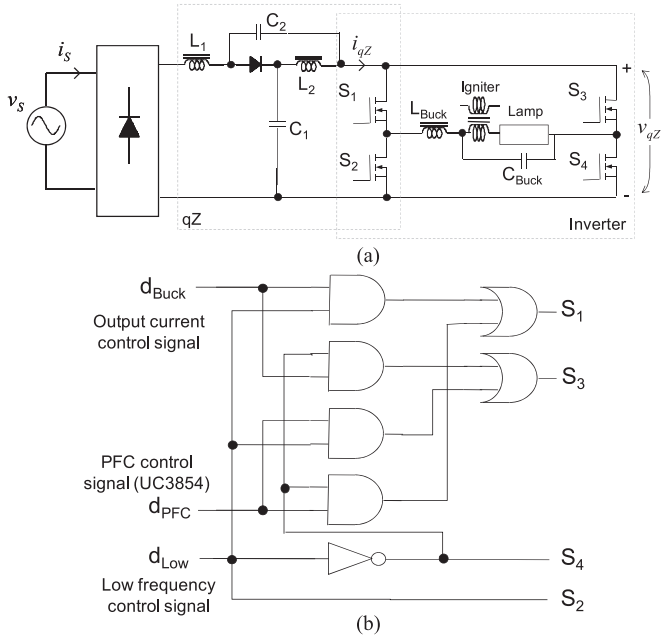


Fig. 6. (a) Electronic ballast based on "qZ" source inverter (a), and (b) the auxiliary combinational circuit.

*3) Controller for the Proposed Z Converter:* Once the converter is designed and the shoot-through state is adjusted, the gate control signals are maintained constant, even during the ignition. Before the ignition, the fluorescent lamp has high impedance, and during this one, the resonant tank provides the needed voltage to turn the lamp ON [21]. The use of an external igniter is not required because the desired output voltage frequency is selected slightly higher than the resonance frequency according to (1).

A microcontroller (PIC16HV616) was employed for the system implementation, which operates at a constant pulse pattern in order to guaranty its performance, as illustrated in Fig. 3.

### *B. Electronic Ballast Based on "qZ" Source Inverter*

Fig. 6(a) illustrates the proposed "qZ" converter, where a full-bridge inverter is implemented and an HID lamp is fed. It consists of four active semiconductors, one diode, the passive elements, and the full-bridge rectifier. An external igniter is used for the lamp ignition.

A circuit UC3854 aids the proposed converter in order to be able to control the input current in CCM to guaranty a high PF. Also, another controller to regulate the output current at low frequency for avoiding acoustic resonance is considered.

The converter operates with a combinational logical circuit as an auxiliary, as shown in Fig. 6(b); $S_1$ and $S_3$ not only regulate the output current, but also correct the PF, the auxiliary circuit allows us to uncouple each controller; $S_2$ and $S_4$ establish the output frequency at which the lamp is operating, which is a square waveform at low frequency.

According to Fig. 7, the converter operates as follows:

1) *During* $t_a - t_b (t_{ST})$. $S_1$, $S_3$, and $S_4$ are turned ON, the equivalent subcircuit is shown in Fig. 8(a), and then a

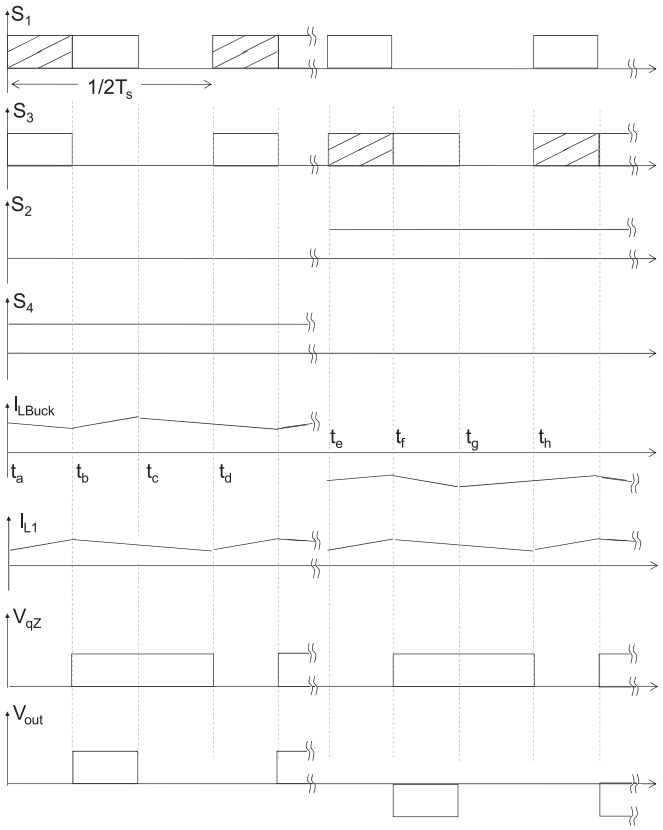


Fig. 7. Output waveform of the "qZ" source inverter.

zero voltage is applied to the lamp, the inverter input voltage is zero ($V_{\rm qZ}$); in this state diode $D_1$ is not conducting, moreover, in this state the inductor $L_1$ current is increasing, this state let us to control the input current and correct the input PF.

2) *During* $t_b - t_c(t_A)$. $S_1$ and $S_4$ are maintained ON, $S_2$ is turned OFF, and the equivalent subcircuit is shown in Fig. 8(b), and then a positive output voltage is delivered to the lamp; the diode is conducting now and the inductor $L_1$ current is decreasing, this state allows controlling the output current and regulating the output power, for the positive semicycle of the output.
3) *During* $t_c - t_d(t_Z)$. $S_4$ is maintained ON, $S_1$ is turned OFF, the equivalent subcircuit is shown in Fig. 8(c), and then a zero voltage is applied to the output filter, the inverter input voltage is zero, the freewheeling diode of $S_2$ is conducting and the inductor $L_1$ current is decreasing.
4) *After* $t_d$. The switching sequences are repeated from this stage until the negative semicycle of the output occurs.
5) *During* $t_e - t_f(t_{ST})$. $S_1$, $S_2$, and $S_3$ are turned ON, $S_4$ is turned OFF, and the equivalent subcircuit is shown in Fig. 8(d), then a zero voltage is still applied to the lamp, $D_1$ is not conducting, and the inductor $L_1$ current is increasing, this state is also used to PF correction.
6) *During* $t_f - t_g(t_A)$. $S_2$ and $S_3$ are maintained ON, and $S_1$ is turned OFF, the equivalent subcircuit is shown in Fig. 8(e), and then a negative voltage is applied to the lamp. This state allows controlling the output current and regulating the output power for the negative semicycle of the output.
7) *During* $t_g - t_h(t_Z)$. Only $S_2$ is maintained ON, the equivalent subcircuit is shown in Fig. 8(f), then a zero voltage is applied to the output filter, the freewheeling diode of $S_4$ is conducting and the inductor $L_1$ current is decreasing.
8) *After* $t_h$. The switching sequences are being repeated since this time, until the negative positive of the output occurs.

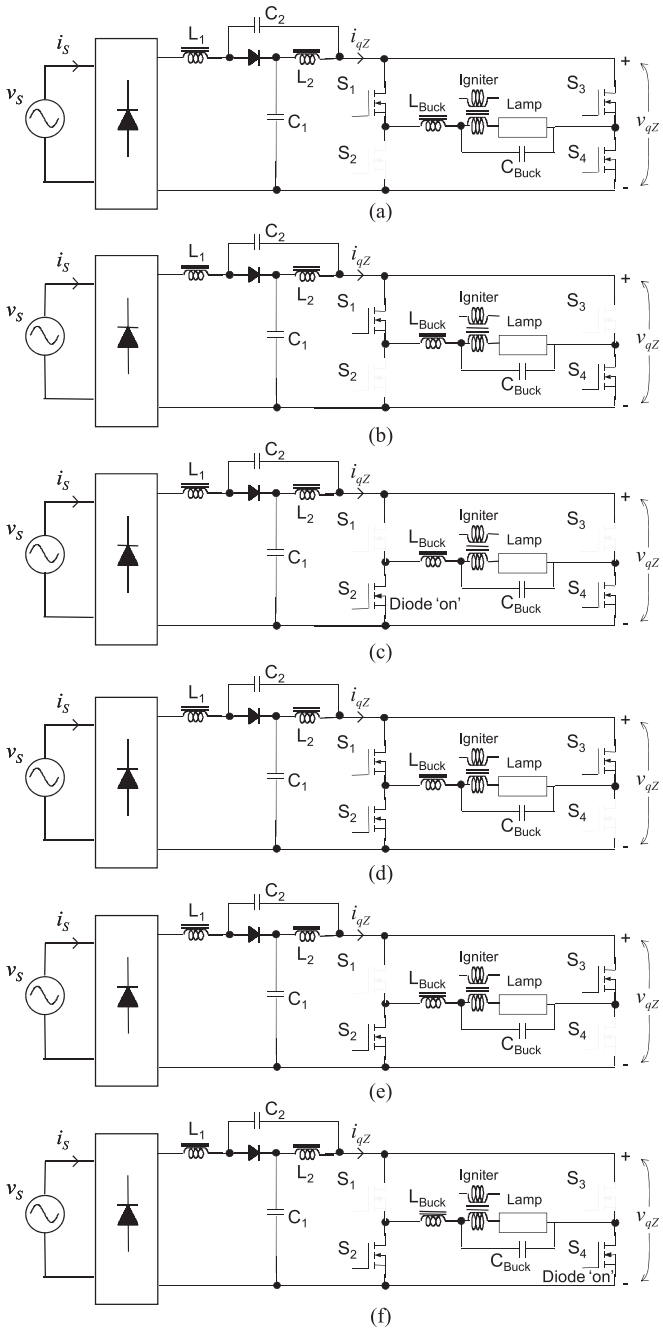


Fig. 8. Subcircuits of the second proposed converter.

Table II summarizes the different switching states of the converter.

*1) Output Characteristics:* For avoiding acoustic resonance at the lamp, the output for the proposed inverter is a

TABLE II
SWITCHING STATES OF THE qZ CONVERTER

| | | Positive Cycle | | | Negative Cycle | | |
|---|---|---|---|---|---|---|---|
| | Switch | $t_{ST}$ | $t_A$ | $t_Z$ | $t_{ST}$ | $t_A$ | $t_Z$ |
| HF | $S_1$ | 1 | 1 | 0 | 1 | 0 | 0 |
| | $S_3$ | 1 | 0 | 0 | 1 | 1 | 0 |
| LF | $S_2$ | 0 | 0 | 0 | 1 | 1 | 1 |
| | $S_4$ | 1 | 1 | 1 | 0 | 0 | 0 |

HF and LF = High/Low Frequency, 0 = Off, 1 = On.

low-frequency square output. A classical controller is employed. The filter is designed taking into account that the ballast operates in high/low-frequency square-wave. This inverter filter is composed by $L_{\rm Buck}$ and $C_{\rm Buck}$, [28], [29], which may be calculated with

$$L_{\rm Buck} = \frac{V_{\rm Lamp}\,(1 - t_A)}{\Delta I_{\rm lamp} F_{\rm switch}} \tag{13}$$

$$C_{\rm Buck} = \frac{\Delta I_{\rm lamp}}{8 F_{\rm switch} \Delta V_{\rm Lamp}} \tag{14}$$

$$t_A = \frac{V_{\rm Lamp}}{V_{\rm Bus}}. \tag{15}$$

where: $L_{\rm Buck}$ inductance of the output filter;
$C_{\rm Buck}$ capacitance of the filter;
$V_{\rm Lamp}$ lamp voltage with the filter;
$T_{\rm switch}$ switching period;
$I_{\rm Lamp}$ lamp current ripple;
$F_{\rm swicth}$ switching frequency;
$V_{\rm Lamp}$ lamp ripple voltage.

The value for the capacitors $C_1$ and $C_2$ are selected to be equal according to [29]–[31], and may be calculated by

$$C_1 = \frac{\sqrt{2} P_{\rm in}}{\omega V_{\rm ACmin}} * \frac{1}{0.05 V_{C1\max}} t_{ST\max} T_{\rm switch} \tag{16}$$

where: $t_{ST\max} = \frac{V_{C1} - V_{\rm in}}{-V_{\rm in} + 2V_{C1}}$:

$V_{C1\max}$ maximum voltage in the capacitor $C_1$;
$P_{\rm in}$ input power of the electronic ballast;
$V_{\rm ACmin}$ minimum input voltage;
$t_{ST\max}$ maximum shoot through state;
$T_{\rm switch}$ switching period.

The selection of the inductors $L_1$ and $L_2$ is based on [28]–[30], and the next equation is used

$$L_1 = L_2 = \frac{V_{C1\max}}{0.2\sqrt{2} P_{\rm in}/V_{\rm ACmin}} t_{ST\max} T_{\rm switch}. \tag{17}$$

*2) Input Characteristics:* The "qZ" array is the inverter input, which is controlled by full bridge inverter. For this particular case, the input inductor $L_1$ is operated in CCM and controlled by the commercial IC UC3854 [32]. This is a specific purpose IC, which allows controlling the converter as a resistance emulator, so that, a PF closer to unity is obtained.

*3) Controller for the Proposed qZ Converter:* Due to the shoot-through state, two controllers, which operate on the same full-bridge inverter, are employed for this converter. An auxiliary circuit is employed in order to uncouple the operation of each controller; as a result, every controller is independent of each other.

The output current operates under a traditional controller, as shown in Fig. 9. It is composed of a rectifier, a PI controller, and a pulse width modulator (PWM). Due to the output ac current, the rectifier is needed.

The input current has a traditional controller with a specific purpose IC; this is known as UC 3854, as illustrated in Fig. 9. The circuit is based on a multiplier and a traditional compensator in order to be able to generate the rectified input current, a current controller, and a PWM, which controls the inductor $L_1$ current. This figure also shows the expected waveform in each point for this controller.

For this converter a traditional external igniter, based on a spark gap, was considered. It was connected in series with the lamp by using a transformer, as shown in Fig. 9.

## III. EXPERIMENTAL RESULTS

The functionality for the proposed systems was experimentally evaluated by a prototype, so that, the proposed ideas were validated.

### A. Electronic Ballast Based on ZSI

Experimental results are shown in Figs. 10–13, these were obtained for a 75-W fluorescent lamp (OSRAM S068 SL75W), the switching frequency is 50 kHz, the resonant tank composed of $L_r$ is 2.17 mH, $C_s$ is 100 nF, and $C_r$ is 5.6 nF, the "Z" inductor $L_Z$ is 190 $\mu$F, and "Z" capacitor $C_Z$ is 47 $\mu$F. A microcontroller PIC16HV616 was used in order to be able to generate the fixed control signals.

Input voltage and current are illustrated in Fig. 10, it is also easily seen that the obtained PF is 0.97 and the total harmonic distortion (THD) of the input current is 14%.

Output waveforms of current and voltage from the lamp are illustrated inFig. 11. It is shown that the output voltage is sinusoidal in spite of being applied a quasi-square output voltage, so that, the lamp is properly fed.

Waveforms from the converter at the switching frequency are illustrated in Fig. 12. It is also shown the inverter input voltage $V_z$, rectified ac mains voltage, and rectified ac mains current. By the time when the capacitor $C_z$ voltage is applied through the inductor $L_z$ to the load, it should be noticed that an oscillation waveform is observed in $V_z$ when the full bridge rectifier is not conducting.

Input waveforms at low frequency from the converter are shown in Fig. 13. This figure also illustrates how the input voltage, rectified ac mains voltage, and inductor current $I_{\rm LZ}$ are in good agreement with the theoretical analysis.

### B. Electronic Ballast Based on "qZ" Source Inverter

A laboratory prototype has been designed, built, and tested for an HID lamp of 250 W (OSRAM HQI-T 250 W/N PLUS), the switching frequency is 50 kHz, the output elements $L_{\rm Buck}$

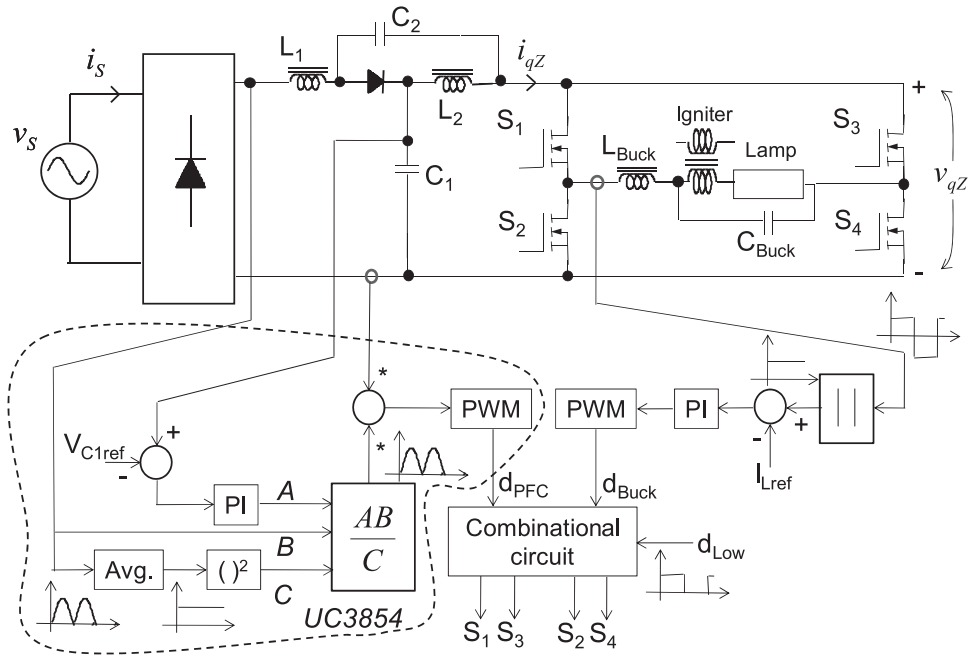


Fig. 9. Controller of the "qZ" source inverter.

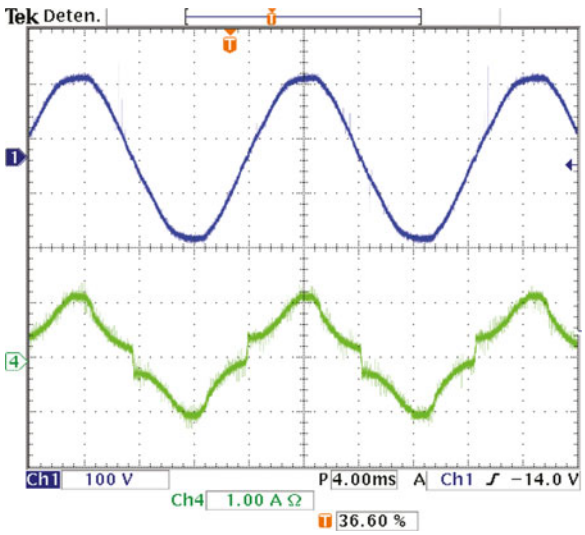


Fig. 10. Input voltage and current (from top to bottom, respectively).

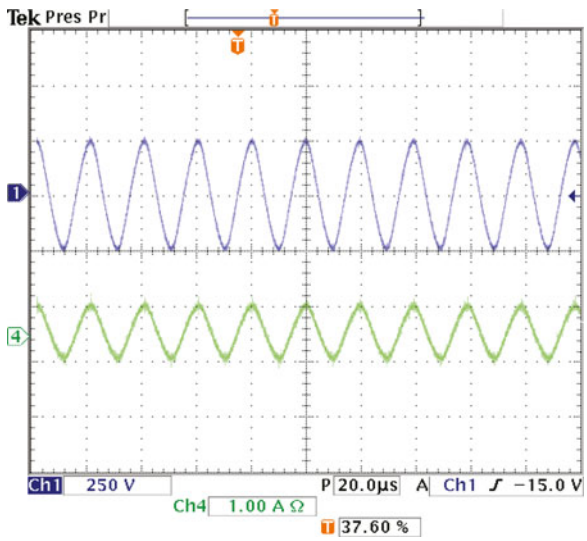


Fig. 11. Voltage and current lamp (from top to bottom, respectively).

is 750 $\mu$H and $C_{\mathrm{Buck}}$ is 500 nF, the "qZ" inductors $L_1$ is 1.2 mF, and "qZ" capacitor $C_1$ is 22 $\mu$F. The IC UC3854 and a logic gates are used in the implementation.

The experimental results are shown in Figs. 14–17. Fig. 14 illustrates the gate signal of the semiconductors which drives the proposed electronic ballast. It also shows the operation under the zero crossing of the output voltage.

The measured waveforms regarding the input current and input voltage are shown in Fig. 15, where the obtained PF is 0.98 and the THD is 12%.

The output waveforms applied to the lamp with a low-frequency square-wave current source are illustrated in Fig. 16. The lamp is driven at low frequency, it is not only free of acoustic resonance and stable, but also the instantaneous power is constant at the lamp.

The startup of the HID lamp is shown in Fig. 17, its waveform has a typical behavior for this loads.

## IV. Conclusion

Different electronic ballasts for lamps are discussed in this paper. The proposal is based on the "Z" and the "qZ" source inverters. Converters offer good input and output characteristics in spite of being used a single stage, which is not an integrated

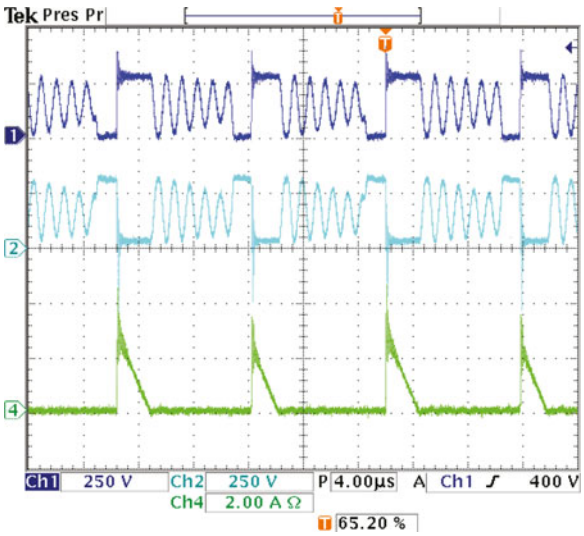


Fig. 12. Inverter input voltage ($V_z$), rectified ac mains voltage and rectified ac mains current.

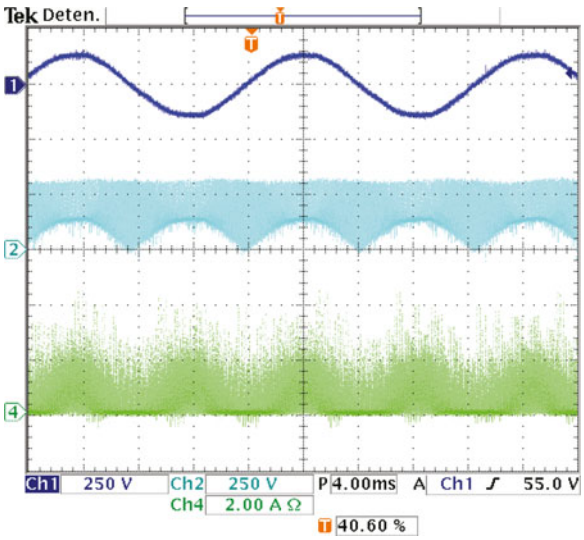


Fig. 13. Input voltage, rectified ac mains voltage, and inductor current ($I_{LZ}$).

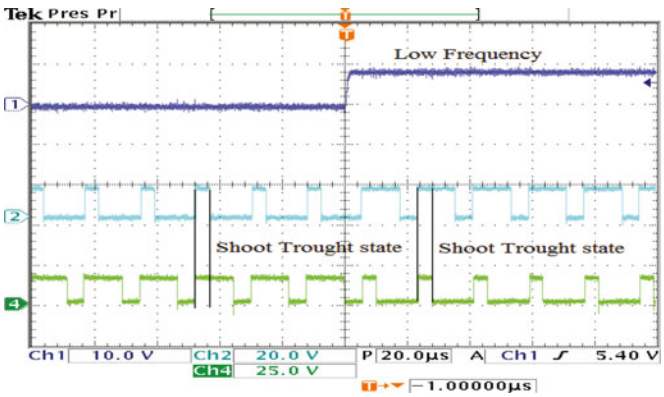


Fig. 14. Gate drive signals. From top to bottom: low-frequency signal ($S_1$), PFC/regulation current gate signal ($S_1$), regulation current/ PFC gate signal ($S_1$). Time scale: 20 $\mu$s/div.

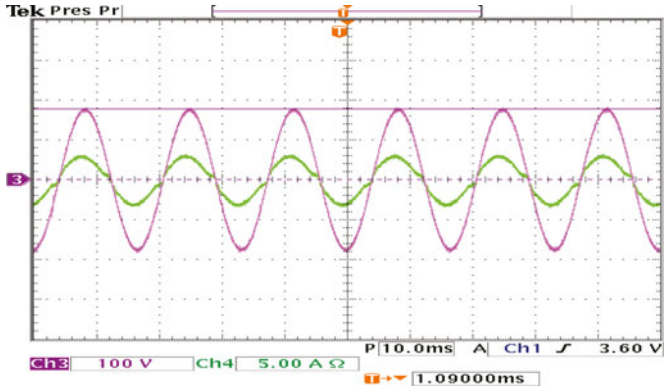


Fig. 15. Input voltage and current. From top to bottom: Input voltage (100 V/div), Input current (5 A/div). Time scale: 10 ms/div.

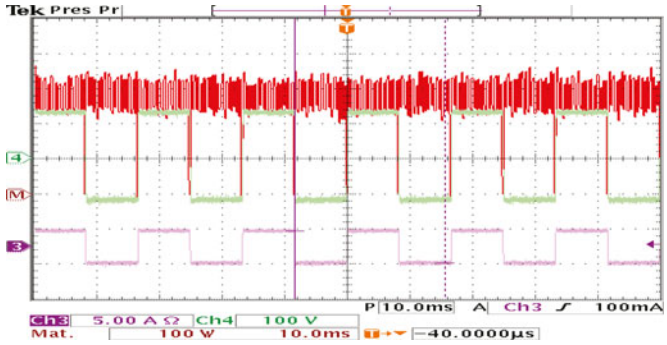


Fig. 16. Waveforms at the lamp. From top to bottom: power lamp (100 W/div), input voltage (100 V/div), lamp current (5 A/div). Time scale: 10 ms/div.

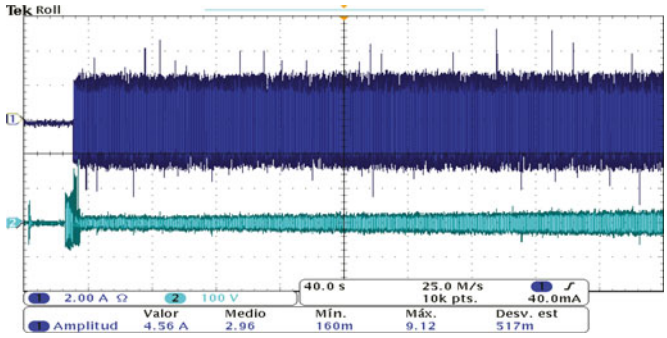


Fig. 17. Start up of the HID lamp.

one. A high PF is obtained and the proper output voltage is applied to the lamp in each case.

Although the "Z" converter inductors are operated in DCM, the "qZ" inductors are operated in CCM; however, these conditions may be switched with its own implications.

The demanded current to the ac mains is similar to that from the converters based on the active input current shaper techniques when operated in DCM, and the current is closer to a sinusoidal waveform when operated in CCM.

The shoot-through state is used not only for boosting the input voltage as typically implemented, but also for obtaining a high PF. The switching states redundancy for the impedance

source converter is used; this enables that two functions may be performed by the same converter.

The operation, analysis, and finally the experimental results were also illustrated.

## REFERENCES


[1] R. Nederson and S. Azzolin, "A high-power-factor electronic ballast using a flyback push–pull integrated converter," *IEEE Trans. Ind. Electron.*, vol. 46, no. 4, pp. 796–892, Aug. 1999.

[2] M. Brumatti, M. Almeida, D.S. L. Simonetti, and J. L. F. Vieira, "Single stage self-oscillating HPF electronic ballast," *IEEE Trans. Ind. Appl.*, vol. 41, no. 3, pp. 735–741, May/Jun. 2005.

[3] C. M. Wang, "A novel single-stage high-power-factor electronic ballast with symmetrical half-bridge topology," *IEEE Trans. Ind. Electron.*, vol. 55, no. 2, pp. 969–972, Feb. 2008.

[4] J. A. Vilela, A. Rodrigues, V. J. Farias, L. C. De Freitas, E. A. Alves, and J. Batista, "An electronic ballast with high power factor and low voltage stress," *IEEE Trans. Ind. Appl.*, vol. 41, no. 4, pp. 917–926, Jul./Aug. 2005.

[5] C. M. Wang, "A novel single-switch single-stage electronic ballast with high input power factor," *IEEE Trans. Power Electron.*, vol. 22, no. 3, pp. 797–803, May 2007.

[6] Y. C. Chuang and H. L. Cheng, "Single-stage single-switch high-power-factor electronic ballast for fluorescent lamps," *IEEE Trans. Ind. Appl.*, vol. 43, no. 6, pp. 1434–1440, Nov./Dec. 2007.

[7] C. S. Moo, K. H. Lee, H. L. Cheng, and W. M. Chen, "A single-stage high-power-factor electronic ballast with ZVS buck–boost conversion," *IEEE Trans. Ind. Electron.*, vol. 56, no. 4, pp. 1136–1146, Apr. 2009.

[8] C. S. Lin and C. L. Chen, "Single-switch electronic ballast with continuous input current charge pump power-factor correction," *IEEE Trans. Ind. Electron.*, vol. 47, no. 6, pp. 1263–1270, Dec. 2000.

[9] H. J. Chiu and S. J. Cheng, "Single-stage voltage source charge-pump electronic ballast with switched-capacitor dimmer for multiple fluorescent lamps," *IEEE Trans. Ind. Electron.*, vol. 54, no. 5, pp. 2915–2918, Oct. 2007.

[10] C. Bitencourt and A. J. Perin, "High power factor electronic ballast for fluorescent lamps with reduced input filter and low cost of implementation," *IEEE Trans. Ind. Electron.*, vol. 55, no. 2, pp. 711–721, Feb. 2008.

[11] J. M. Alonso, M. A. Dalla, M. Rico-Secades, J. Cardesín, and J. García, "Investigation of a new control strategy for electronic ballasts based on variable inductor," *IEEE Trans. Ind. Electron.*, vol. 55, no. 1, pp. 3–10, Jan. 2008.

[12] M. S. Perdigão, J. M. Alonso, M. A. Dalla, and E. Sousa, "Comparative analysis and experiments of resonant tanks for magnetically controlled electronic ballasts," *IEEE Trans. Ind. Electron.*, vol. 55, no. 9, pp. 3201–3211, Sep. 2008.

[13] S. Borekci, "Dimming electronic ballasts without striations," *IEEE Trans. Ind. Electron.*, vol. 56, no. 7, pp. 2464–2468, Jul. 2009.

[14] Á. Raniere, F. Ecke, and R. Nederson, "A design methodology for a self-oscillating electronic ballast," *IEEE Trans. Ind. Appl.*, vol. 43, no. 6, pp. 1254–1533, Nov./Dec. 2007.

[15] H.-L. Do, K.-W. Seok, and B.-H. Kwon, "Single-stage electronic ballast with unity power factor," *Proc. IEE Elect. Power Appl.*, vol. 448, no. 2, pp. 171–176, Mar. 2001.

[16] S. Miaosen, Q. Zhaoming, and P. Fang, "Design of a two-stage low-frequency squarewave electronic ballast for HID lamps," *IEEE Trans. Ind. Appl.*, vol. 39, no. 2, pp. 424–430, Jul./Aug. 2003.

[17] C. Chun-An and C.-W. Ku, "A novel single-stage cost-effective electronic ballast for HID lamps with high power factor," in *Proc. IEEE 8th Int. Conf. Publ. Power Electron. ECCE Asia*, 2011, pp. 795–802.

[18] F. T. Wakabayashi and C. A. Canesin, "An improved design procedure for LCC resonant filter of dimmable electronic ballasts for fluorescent lamps, based on lamp model," *IEEE Trans. Power Electron.*, vol. 20, no. 5, pp. 1186–1196, May 2005.

[19] J. Cardesín, J. García, J. Ribas, J. M. Alonso, A. J. Calleja, E. L. Corominas, M. Rico-Secades, and M. Dalla, "Low-cost PFC electronic ballast for 250W HID lamps operating as constant power source with 400 kHz switching frequency," in *Proc. Power Electron. Spec. Conf.*, 2005, pp. 1130–1135.

[20] J. A. Vilela, A. Rodrigues, V. J. Farias, L. C. De Freitas, E. A. Alves, and J. Batista, "An electronic ballast with high power factor and low voltage stress," *IEEE Trans. Ind. Appl.*, vol. 41, no. 4, pp. 917–926, Jul./Aug. 2005.

[21] L. Ray-Lee and L. Chih, "Design and implementation of novel Single-stage charge-pump power-factor-correction electronic ballast for metal halide lamp," *IEEE Trans. Ind. Electron.*, vol. 59, no. 4, pp. 1789–1798, Apr. 2012.

[22] F. Z. Peng, "Z-source inverter," *IEEE Trans. Ind. Appl.*, vol. 39, no 2, pp. 504–510, Mar./Apr. 2003.

[23] I. Roasto, D. Vinnikov, T. Jalakas, J. Zakis, and S. Ott, "Experimental study of shoot-through control methods for qZSI-based DC/DC converters," in *Proc. Int. Symp. Power Electron. Elect. Drives Autom. Motion*, 2010, pp. 29–34.

[24] Y. P. Siwakoti, P. C. Loh, F. Blaabjerg, and G. E. Town, "Y-source impedance network," *IEEE Trans. Power Electron.*, vol. 29, no. 7, pp. 3250–3254, Jul. 2014.

[25] C. Xia and X. Li, "Z-source inverter-based approach to the zero-crossing point detection of back EMF for sensorless brushless DC motor," *IEEE Trans. Power Electron.*, vol. 30, no. 3, pp. 1488–1498, Mar. 2015.

[26] V. Fernao Pires, A. Cordeiro, D. Foito, and J. F. Martins, "Quasi-Z-source inverter with a T-type converter in normal and failure mode," *IEEE Trans. Power Electron.*, to be published, DOI:10.1109/TPEL.2016.2514979

[27] N. Vázquez, H. López, C. Hernández, E. Vázquez, R. Osorio, and J. Arau, "A different multilevel current source inverter," *IEEE Trans. Ind. Electron.*, vol. 57, no. 8, pp. 2623–2632, Aug. 2010.

[28] K. Beer and B. Piepenbreier, "Properties and advantages of the quasi-Z-source inverter for DC–AC conversion for electric vehicle applications," in *Proc. Int. Conf. Anti-Counterfeiting, Security Identification*, 2010, pp. 1–6.

[29] L. Yuan and Z. Peng, "AC small signal modeling, analysis and control of quasi-Z-source converter," in *Proc. 7th Int. Power Electron. Motion Control Conf.*, 2012, vol. 3, pp. 1848–1854.

[30] STMicroelectronics, Appl. Note 2747, pp. 1–44, 2008.

[31] L. Chun, P. Maussion, S. Bhosle, and G. Zissis, "Characterization of acoustic resonance in a high pressure sodium lamp," *IEEE Trans. Ind. Appl.*, vol. 47, no. 2, pp. 1071–1076, Mar./Apr. 2011.

[32] Unitrode UC3854, Appl. Note 134, pp. 269–328, 1999.


**Nimrod Vázquez** (M'98–SM'11) was born in Mexico City, Mexico, in 1973. He received the B.S. degree in electronics engineering from the Instituto Tecnológico de Celaya, Celaya, Mexico, in 1994, the M.Sc. degree in electronics engineering and the Dr. Ing. degree from the Centro Nacional de Investigación y Desarrollo Tecnológico, Cuernavaca, Mexico, in 1997 and 2003, respectively.

Since 1998, he has been with the Department of the Electronics Engineering, Instituto Tecnológico de Celaya. His research interests include uninterruptible power supplies, dc/ac converters, power-factor correction, nonlinear control techniques, and renewable energy.

**Edgar Baeza** was born in San José Iturbide, Mexico, in 1988. He received the B.S. degree in mechatronics engineering from the Universidad Tecnológica del Norte de Guanajuato, Dolores Hidalgo, Mexico, in 2011, and the M.Sc. degree in electronics engineering from InstitutoTecnológico de Celaya, Celaya, Mexico, in 2014.

Since 2014, he has been with the Department of the Electronics Engineering, Universidad Tecnológica del Norte de Guanajuato. His research interests include electronic ballasts, dc/dc and dc/ac converters, and renewable energy.

**Alejandro Perea** was born in Celaya, Guanajuato, in 1984. He received the B.S. degree in electronics engineering and the M.Sc. degree in electronics engineering from the Instituto Tecnológico de Celaya, Celaya, Mexico, in 2008 and 2011, respectively.

Since 2011, he has been working on new projects engineering at Mariscala P&G and Nestlé-Purina León plants, León, Mexico. His research interests include drive controllers, PLC, MCC, safety circuits, communications systems, lighting, and renewable energy.

**Claudia Hernández** (M'98) was born in Salamanca, Mexico, in 1971. She received the B.S. degree from the Celaya Institute of Technology, Celaya, Mexico, in 1995, and the M.Sc. degree in electronics engineering from the Centro Nacional de Investigacion y Desarrollo Tecnologico, Cuernavaca, México, in 2000, both in electronics engineering.

Since 1998, she has been with the Department of Electronics Engineering, Instituto Tecnológico de Celaya. Her research interests include dc/ac converters, power factor correction, and active filters.

**Eslí Vázquez** was born in Mexico City, Mexico, in 1969. He received the B.S. degree from the Celaya Institute of Technology, Celaya, Mexico, the M.Sc. degree from the Autónoma Metropolitana–Iztapalapa University, Mexico, and the Ph.D. degree from the Imperial College London, London, U.K.

He is currently a Lecturer at the Veracruzana University, Xalapa, Mexico.

**Héctor López** received the M.Sc. degree from the University of Birmingham and Nottingham, Nottingham, U.K., in 2002, and the Ph.D. degree from the University of San Luis Potosí, San Luis Potosí, Mexico, in 2008, both in electrical engineering.

He is currently a Professor at the Department of Electronic Engineering, Celaya Institute of Technology, Guanajuato, Mexico. He is also an Adjunct Assistant Professor at the Mechanical Department, McMaster University, Hamilton, ON, Canada. His research interests include power electronics, electric motor drives, renewable energy, smart grid, energy conversion systems, and transportation electrification.